SCIENCE CHINA
Technological Sciences

• Article •

February 2016 Vol.60 No.2: 199–208
doi: 10.1007/s11431-016-0423-9

Robust control for active suspension system under steering condition

WANG ChunYan[1], DENG Ke[1], ZHAO WanZhong[1*], ZHOU Guan[1] & LI XueSong[2]

[1] *Department of Automotive Engineering, Nanjing University of Aeronautics and Astronautics, Nanjing 210016, China;*
[2] *State Key Laboratory of Automobile Simulation and Control, Jilin University, Changchun 130025, China*

Received May 27, 2016; accepted September 12, 2016; published online November 2, 2016

To minimize the auto body's posture change caused by steering and uneven road, and improve the vehicle's riding comfort and handling stability, this paper presents an H_∞ robust controller of the active suspension system, which considers the effects of different steering conditions on its dynamic performance. The vehicle's vibration in the yaw, roll, pitch and vertical direction and the suspension's dynamic deflection in the steering process are taken into account for the designed H_∞ robust controller, and it introduces the frequency weight function to improve the riding comfort in the specific sensitive frequency bands to human body. The proposed robust controller is testified through simulation and steering wheel angle step test. The results show that the active suspension with the designed robust controller can enhance the anti-roll capability of the vehicle, inhibit the changes of the body, and improve the riding comfort of the vehicle under steering condition. The results of this study can provide certain theoretical basis for the research and application of active suspension system.

vehicle, active suspension system, steering condition, H_∞ robust control, sensitive frequency bands

Citation: Wang C Y, Deng K, Zhao W Z, et al. Robust control for active suspension system under steering condition. Sci China Tech Sci, 2017, 60: 199–208, doi: 10.1007/s11431-016-0423-9

1 Introduction

The suspension system is one of the important components of the chassis system of the vehicle, whose function is to transfer the force and torque between the wheels and the frame, ease the impact load caused by uneven pavement, and attenuate the vibration of the bearing system. Therefore, the performance of the suspension system directly affects the vehicle's smoothness and handling stability [1,2]. Compared with the passive suspension system, the stiffness and damping characteristics of the active suspension system can be adjusted dynamically according to the driving condition of the vehicle, so that the vehicle has better riding comfort and handling stability.

Many scholars have studied the active suspension system, and the research contents are mainly focused on using different control methods to improve the body posture and the change of dynamic load between the wheels and road surface, and further enhance the vehicle's riding comfort and handling stability. Nowadays, fuzzy control, optimal control, adaptive control, etc., are applied to the active suspension system.

Fuzzy control [3–9] method does not need to establish an accurate model of the control object. It always takes the vertical acceleration, relative velocity of the body and relative speed of the wheel as inputs to control the active suspension by actuator. Optimal control [10–13] method obtains the optimal control input through a certain mathematical method as the performance evaluation function selecting the extreme value. Adaptive control [14,15] method always

*Corresponding author (email: zhaowanzhong@126.com)

considers the variability of the parameters of the active suspension system, and can identify the system state according to the conditional variant. Thus, it can keep the best ability to adapt to the current state.

Throughout the published literatures, it can be seen that most studies about the active suspension system have not considered the effects of different steering conditions on the dynamic performance of the active suspension system, that is, they separate the influence of them on riding comfort and handling stability of the vehicle. However, as shown in Figure 1, the active suspension system and steering system are always influenced by each other [16]. For example, the vehicle is often in different steering states in the driving process, and the horizontal vibration caused by side lurch in the steering process has a great influence on the occupant comfort and vehicle stability. Therefore, it is necessary to take the steering condition into account in the controller design of the active suspension system.

Moreover, the controller of the active suspension system is prone to be influenced by road disturbance [17], parameter perturbation, the error between the real and measured vehicle dynamics [18], and so on. These uncertainty effects always lead to performance deterioration, or even failure of the controller. In order to ensure the control object working in accordance with the predetermined goal, robust control methods should be used to make the active suspension system keep robust stability from uncertainty, and maintain good robustness.

In addition, according to ISO2631-1:1997 (E) standards, the human body is sensitive to the vertical vibration of 4–8 Hz and horizontal vibration of 1–2 Hz. And the papers gave the finite frequency results that the human body is more sensitive to vibrations of 4–8 Hz in the vertical direction [19,20]. However, the existing controller design of active suspension system rarely takes into account the performance requirements in the frequency domain. Especially in the specific frequency range of 4–8 Hz and 1–2 Hz, the performance of the active suspension is even worse than the passive suspension, which will reduce the riding comfort in a large extent.

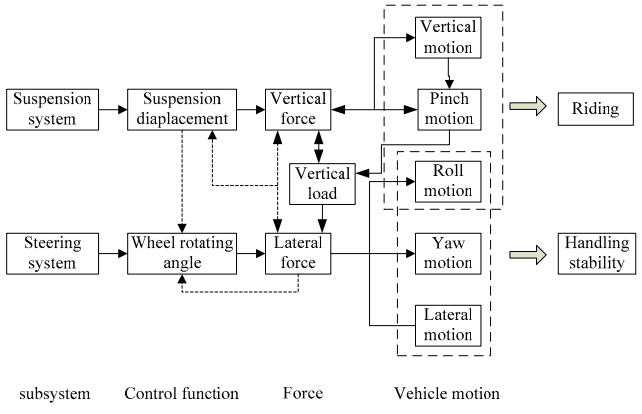

Figure 1 Relationship between suspension and steering system.

To address the above-mentioned problems, this paper presents a robust controller of the active suspension system under steering condition, which considers the most sensitive frequency bands to the human body. The corresponding vibration is conducted by frequency weight as the evaluating index of comfort. The rest of this paper is organized as follows: The dynamic model of the active suspension system, tire model and road input model are established in Section 2. In Section 3, considering the robustness of the active suspension system, an H_∞ robust controller is designed based on generalized system with frequency weighting. Simulations under different front wheel angles, random road inputs and amplitude-frequency characteristic are carried out in Section 4. Section 5 further presents the steering wheel angle step input test, and conclusions are given in Section 6.

2 Dynamic model

2.1 Dynamic model of active suspension

In this paper, the effects of the crosswind force and its corresponding torque on the vehicle are ignored, and it is assumed that the tire has a linear characteristic under small steering angles. The vehicle does lateral and yaw movement when steering, whose steering state model is shown in Figure 2, and the model of active suspension system is shown in Figure 3.

Considering the influence of the body roll movement, the differential equation of lateral and yaw directions for the vehicle can be expressed as:

$$mu\left(\omega_r+\dot{\beta}\right)-m_2h\ddot{\phi}=F_{YA}+F_{YB}+F_{YC}+F_{YD}, \tag{1}$$

$$I_z\dot{\omega}_r=a(F_{YA}+F_{YB})-b(F_{YC}+F_{YD}), \tag{2}$$

where m is the vehicle total mass; m_2 is the sprung mass; u is the vehicle velocity; β is the sideslip angle; ω_r is the yaw rate; h is the height of the roll center; ϕ is body roll angle; F_{YA}, F_{YB}, F_{YC}, F_{YD} are the lateral force of the left front, right front, left rear and right rear tires, respectively; I_Z is the yaw moment of inertia of the vehicle; a, b are the distance of front and rear axle to center of mass, respectively.

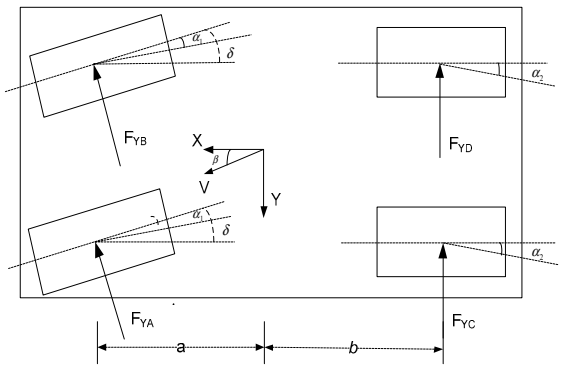

Figure 2 Vehicle steering state model.

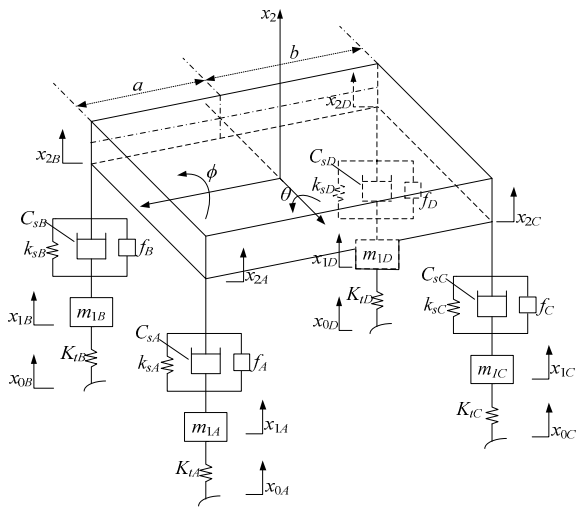

Figure 3 Active suspension system model.

The differential equation of the body pitch motion can be written as:

$$I_{\mathrm{p}}\ddot{\theta} = b(F_C + F_D) - a(F_A + F_B), \tag{3}$$

where I_{p} is the body pitch moment of inertia; θ is the body pitch angle; F_A, F_B, F_C, F_D are the vertical force acting on the body at each suspension point, respectively.

The differential equation of the body roll motion can be written as:

$$I_{\mathrm{r}}\ddot{\phi} = m_2 u\left(\omega_r + \dot{\beta}\right)h + m_2 g h\phi + (F_A + F_C - F_B - F_D)t, \tag{4}$$

where I_{r} is the body roll moment of inertia; ϕ is the body roll angle.

The vertical movement of the suspended mass can be written as:

$$m_2\ddot{x}_2 = F_A + F_B + F_C + F_D, \tag{5}$$

where m_2 is the sprung mass; x_2 is vertical displacement of the suspension center of mass.

The vertical movement of the non-suspended mass can be given as:

$$m_{1i}\ddot{x}_{1i} = k_{ti}\left(x_{0i} - x_{1i}\right) - F_i, \quad i = A, B, C, D, \tag{6}$$

$$\begin{cases} F_A = k_{\mathrm{s}A}(x_{1A} - x_{2A}) + c_{\mathrm{s}A}(\dot{x}_{1A} - \dot{x}_{2A}) \\ -\dfrac{k_{\mathrm{af}}}{2t}(\phi - \dfrac{x_{1A} - x_{1B}}{2t}) + f_A, \\ F_B = k_{\mathrm{s}B}(x_{1B} - x_{2B}) + c_{\mathrm{s}B}(\dot{x}_{1B} - \dot{x}_{2B}) \\ +\dfrac{k_{\mathrm{af}}}{2t}(\phi - \dfrac{x_{1A} - x_{1B}}{2t}) + f_B, \\ F_C = k_{\mathrm{s}C}(x_{1C} - x_{2C}) + c_{\mathrm{s}C}(\dot{x}_{1C} - \dot{x}_{2C}) \\ -\dfrac{k_{\mathrm{ar}}}{2t}(\phi - \dfrac{x_{1C} - x_{2D}}{2t}) + f_C, \\ F_D = k_{\mathrm{s}D}(x_{1D} - x_{2D}) + c_{\mathrm{s}D}(\dot{x}_{1D} - \dot{x}_{2D}) \\ +\dfrac{k_{\mathrm{ar}}}{2t}(\phi - \dfrac{x_{1C} - x_{1D}}{2t}) + f_D, \end{cases} \tag{7}$$

where $m_{1i}(i = A, B, C, D)$ is each non-suspended mass; $x_{1i}(i = A, B, C, D)$ is the vertical displacement of each non-suspended mass; $x_{0i}(i = A, B, C, D)$ is the road input excitation of each tire; $x_{2i}(i = A, B, C, D)$ is the vertical displacement of the suspended mass at each suspension point; $k_{ti}(i = A, B, C, D)$ is each tire stiffness; $k_{si}(i = A, B, C, D)$ is the suspension stiffness at each wheel; $c_{si}(i = A, B, C, D)$ is the suspension damping coefficient at each wheel; k_{af}, k_{ar} are the angular stiffness of the lateral stabilizer bar of the front and rear suspension, respectively; $f_i(i = A, B, C, D)$ is the force of each active suspension actuators.

When θ and ϕ are smaller, the vertical displacement of the four wheels can be expressed as:

$$\begin{cases} x_{2A} = x_2 - a\theta + t\phi, \\ x_{2B} = x_2 - a\theta - t\phi, \\ x_{2C} = x_2 + b\theta + t\phi, \\ x_{2D} = x_2 + b\theta - t\phi. \end{cases} \tag{8}$$

2.2 Tire model

Neglecting the effect of the aligning torque and the load change on the characteristics of the tire, it can be considered to be linear in a small steering angle condition. The cornering force of the tire can be expressed as:

$$\begin{cases} F_{YA} = F_{YB} = k_1\alpha_1, \\ F_{YC} = F_{YD} = k_2\alpha_2, \end{cases} \tag{9}$$

where $\alpha_1 = \delta + E_{\mathrm{f}}\phi - \beta - \dfrac{a\omega_r}{u}$ and $\alpha_2 = \dfrac{b\omega_r}{u} + E_{\mathrm{r}}\phi - \beta$; δ is the steering angle of the front wheel; k_1 and k_2 are the cornering stiffness of the front and rear wheels, respectively; α_1 and α_2 are the sideslip angles of the front and rear wheels, respectively; E_f and E_r are the roll steering coefficients of the front and rear wheels.

2.3 Road input model

As the vehicle vibration input, the statistical properties of the road roughness is used to describe the road power spectral density. The road input to wheel is filtered white noise, that is [21]

$$\dot{x}_{0i} = -2\pi f_0 x_{0i} + 2\pi\sqrt{G_0 u}\,\omega_{0i}(t), \tag{10}$$

where f_0 is the lower cutoff frequency; G_0 is the road roughness; $w_{0i}(t)$ is the Gauss white noise of zero mean; u is the speed of the vehicle.

It is assumed that the road input excitation of the left and right wheels are not relevant, and the time delay $T = \dfrac{a+b}{u}$

between the front and rear wheel is due to the wheelbase. Thus, the following equation can be got: $w_{03}(t)=w_{01}(t-T)$, $w_{04}(t)=w_{02}(t-T)$.

3 H_∞ robust controller design under steering condition

3.1 General structure of H_∞ control system

H_∞ control [22] is an effective method to design the controller of uncertain system. It takes the H_∞ norm of the transfer function from disturbance input to system output the as objective function to optimize the system, which can minimize the effect of the disturbance on system output [23]. Thus, the controller designed by H_∞ control has good robust stability.

The general structure of the H_∞ robust control system is shown in Figure 4.

In Figure 4, $G_0(s)$ is a linear time invariant system, whose state space can be expressed as:

$$\begin{cases} \dot{\boldsymbol{x}} = A\boldsymbol{x} + B_1\boldsymbol{w} + B_2\boldsymbol{u}, \\ \boldsymbol{z} = C_1\boldsymbol{x} + D_{11}\boldsymbol{w} + D_{12}\boldsymbol{u}, \\ \boldsymbol{y} = C_2\boldsymbol{x} + D_{21}\boldsymbol{w} + D_{22}\boldsymbol{u}, \end{cases} \tag{11}$$

where $\boldsymbol{x}\in R^n$ is the state vector; $\boldsymbol{u}\in R^m$ is the control input vector; $\boldsymbol{y}\in R^p$ is the measurement output matrix; $\boldsymbol{z}\in R^r$ is the controlled output matrix; $\boldsymbol{w}\in R^q$ is the input vector of the external disturbance; K(s) is the transfer function of the controller.

Therefore, the system control problem can be expressed as:

$$\begin{bmatrix} \boldsymbol{z} \\ \boldsymbol{y} \end{bmatrix} = G_0(s)\begin{bmatrix} \boldsymbol{w} \\ \boldsymbol{u} \end{bmatrix} = \begin{bmatrix} G_{11}(s) & G_{12}(s) \\ G_{21}(s) & G_{22}(s) \end{bmatrix}\begin{bmatrix} \boldsymbol{w} \\ \boldsymbol{u} \end{bmatrix}. \tag{12}$$

The purpose of the H_∞ control system is to design a controller $u(s)=k(s)y(s)$, which can make the closed-loop system satisfy the following requirements: (1) The internal stability of the closed-loop system. (2) The H_∞ norm of the closed-loop transfer function $T_{wz}(s)$ from the disturbance input w to the controlled output Z is less than 1, that is, $\|T_{wz}(s)\|_\infty < 1$.

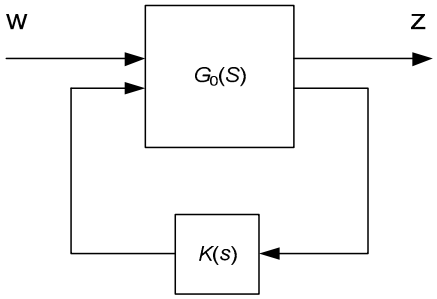

Figure 4 General structure of the H_∞ robust control system.

3.2 H_∞ control model under steering condition

In this paper, the H_∞ closed-loop control system with weighted output feedback is designed based on the established dynamic models in Section 2.

The state variable of the system is chosen as:

$$\begin{aligned} \boldsymbol{x} = [&x_2, \dot{x}_2, \phi, \dot{\phi}, \theta, \dot{\theta}, \dot{x}_{1A}, \dot{x}_{1B}, \dot{x}_{1C}, \dot{x}_{1D}, x_{1A}, \\ &x_{1B}, x_{1C}, x_{1D}, \omega_r, \beta]^{\mathrm{T}}. \end{aligned} \tag{13}$$

The control input of the system is written as:

$$\boldsymbol{u} = [f_A, f_B, f_C, f_D]^{\mathrm{T}}. \tag{14}$$

The interference input of the system is defined as:

$$\boldsymbol{w} = [\delta, x_{0A}, x_{0B}, x_{0C}, x_{0D}]^{\mathrm{T}}. \tag{15}$$

The controlled output of the system is given as:

$$\begin{aligned} \boldsymbol{z} = [&\ddot{x}_2, \ddot{\phi}, \ddot{\theta}, x_{2A} - x_{1A}, x_{2B} - x_{1B}, x_{2C} - x_{1C}, x_{2D} - x_{1D}, \\ &x_{0A} - x_{1A}, x_{0B} - x_{1B}, x_{0C} - x_{1C}, x_{0D} - x_{1D}, f_A, f_B, f_C, f_D]^{\mathrm{T}}. \end{aligned} \tag{16}$$

The measurement output of the system is expressed as:

$$\boldsymbol{y} = [\ddot{x}_2, \dot{\phi}, \dot{\theta}]^{\mathrm{T}}. \tag{17}$$

Then, the state space equations of the suspension system can be depicted as:

$$\begin{cases} \dot{\boldsymbol{x}} = \boldsymbol{A}\boldsymbol{x} + \boldsymbol{B}_1\boldsymbol{w} + \boldsymbol{B}_2\boldsymbol{u}, \\ \boldsymbol{z} = \boldsymbol{C}_1\boldsymbol{x} + \boldsymbol{D}_{11}\boldsymbol{w} + \boldsymbol{D}_{12}\boldsymbol{u}, \\ \boldsymbol{y} = \boldsymbol{C}_2\boldsymbol{x} + \boldsymbol{D}_{21}\boldsymbol{w} + \boldsymbol{D}_{22}\boldsymbol{u}. \end{cases} \tag{18}$$

The above equations can be written as:

$$\boldsymbol{G}_0(s) = \boldsymbol{C}(s\boldsymbol{I} - \boldsymbol{A})^{-1}\boldsymbol{B} + \boldsymbol{D}, \tag{19}$$

where $\boldsymbol{A}$ is the state matrix with 16×16 dimension; $\boldsymbol{B}_1$ is the interference input matrix with 16×5 dimension; $\boldsymbol{B}_2$ is the control input matrix with 16×4 dimension; $\boldsymbol{C}_1$ is the controlled state matrix with 15×16 dimension; $\boldsymbol{D}_{11}$ is the controlled interference input matrix with 15×5 dimension; $\boldsymbol{D}_{12}$ is the controlled input matrix with 15×4 dimension; $\boldsymbol{C}_2$ is the measurement state matrix with 3×16 dimension; $\boldsymbol{D}_{21}$ is the measurement interference input matrix with 3×5 dimension; $\boldsymbol{D}_{22}$ is the measurement input matrix with 3×4 dimension.

3.3 Weight function

The block diagram of H_∞ closed-loop control system with weighted output feedback is shown in Figure 5.

Generally speaking, the time domain responses of the system's state variables are always taken as control index, which means the vibration states and input energy of the

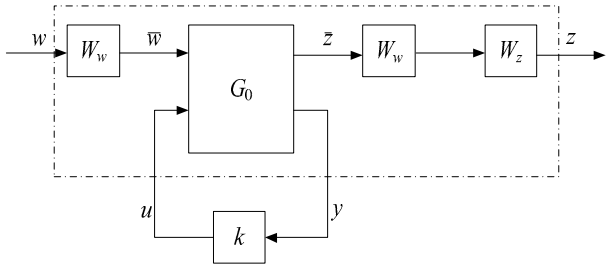

Figure 5 Block diagram of the designed H_∞ control system.

system in different frequency bands are controlled equally. However, for the vertical, pitch and roll vibration of reflecting the riding comfort, the sensitive degrees of the human body in different frequency bands are not the same.

According to ISO2631-1:1997 (E) standards, the human body is sensitive to the vertical vibration of 4–12.5 Hz and horizontal vibration of 1–2 Hz. In order to improve the ride comfort in the two specific frequency ranges, the corresponding weight function is selected as follows [24,25]:

$$W_1(s)=\frac{s^2+100s+987}{s^2+44s+987}, \tag{20}$$

$$W_2(s)=\frac{s^2+50.27s+25.72}{s^2+7.037s+25.72}. \tag{21}$$

The weighting transfer function matrix of the controlled output is defined as:

$$\boldsymbol{W}_P=\mathrm{diag}(W_1,W_2,W_2,1,1,1,1,1,1,1,1,1,1,1,1). \tag{22}$$

The weighting coefficient matrix of the interference input is written as:

$$\boldsymbol{W}_w=\mathrm{diag}(0.0001,0.0001,0.0001,0.0001,0.0001). \tag{23}$$

The weighting coefficient matrix of the controlled output is given as:

$$\begin{aligned}\boldsymbol{W}_z=\mathrm{diag}(&5,1,1,25,25,25,25,25,25,25,25,\\&0.0155,0.0155,0.0155,0.0155).\end{aligned} \tag{24}$$

Therefore, the generalized controlled object of the active suspension system under the steering condition can be expressed as follows:

$$\begin{bmatrix}\boldsymbol{z}\\ \boldsymbol{y}\end{bmatrix}=G_0(s)\begin{bmatrix}\boldsymbol{w}\\ \boldsymbol{u}\end{bmatrix}=\begin{bmatrix}\boldsymbol{W}_z\boldsymbol{W}_pG_{11}(s)\boldsymbol{W}_w & \boldsymbol{W}_z\boldsymbol{W}_pG_{12}(s)\\ G_{21}(s)\boldsymbol{W}_w & G_{22}(s)\end{bmatrix}\begin{bmatrix}\boldsymbol{w}\\ \boldsymbol{u}\end{bmatrix}. \tag{25}$$

It can be validated that the system is a 16 order controllable one. Thus, the problem of the controller design is converted into the standard H_∞ controller of the generalized system containing the weighting function. The controller $\boldsymbol{K}=\boldsymbol{C}_k(s\boldsymbol{I}-\boldsymbol{A})^{-1}\boldsymbol{B}_k+\boldsymbol{D}_k$ can be solved by MATLAB/LMI toolbox, and the following condition should be satisfied: $\left\|T_{\overline{wz}}(s)\right\|_\infty<1$.

4 Simulation analysis

In this paper, the simulation models of the controller and the active suspension system are established with MATLAB/Simulink software. The simulations are carried out with different front wheel angles and random road inputs in steering condition, and the simulation results of the active suspension with H_∞ robust controller are compared with LQR controller and the passive suspension to verify the control effect. Table 1 shows the main simulation parameters.

4.1 Step input simulation under different front wheel angles

Setting the initial speed of the vehicle as 20 m/s, the front wheel angle δ as the step input of 6° and 10°, and the road condition as *B*-class, the simulation results of active suspension with H_∞ and LQR control respectively, and passive suspension are shown in Figures 6–9.

From Figures 6–9, the following conclusions can be got:

(1) In comparison with the passive suspension, the active suspension can efficiently reduce the vehicle vertical acceleration, roll angle acceleration, pitch angle acceleration and suspension dynamic deflection. So it can better buffer the vibration impact from the road, and improve the riding comfort of the vehicle.

(2) Under any of the two control methods, the dynamic overshoot of the vehicle vertical acceleration and pitch angle acceleration between the two front wheel angle inputs

Table 1 Main simulation parameters

Name	Value	Name	Value
Vehicle total mass m (kg)	1985	Moment of inertia of vehicle around Z axis I_Z (kg m^2)	2850
Sprung mass m_2 (kg)	1500	Moment of inertia of vehicle around X axis I_P (kg m^2)	2460
Non-sprung mass m_{1A}(m_{1B}, m_{1C}, m_{1D}) (kg)	59	Moment of inertia of vehicle around Y axis I_r (kg m^2)	760
Distance from front axle to center of mass a (m)	1.36	Front suspension stiffness k_{SA} (k_{SB}) (N m^{-1})	35500
Distance from rear axle to center of mass b (m)	1.78	Rear suspension stiffness k_{SC} (k_{SD}) (N m^{-1})	38500
Tire stiffness k_{ta} (k_{ta}, k_{ta}, k_{ta}) (N m^{-1})	129000	Front suspension damping coefficient c_{SA} (c_{SB}) (N s m^{-1})	1200
Tire cornering stiffness k_1(k_2) (N rad^{-1})	35000	Rear suspension damping coefficient c_{SC} (c_{SD}) (N s m^{-1})	1100
Lateral stable pole angle stiffness K_{af}(k_{ar}) (N m rad^{-1})	6695	Half of wheelbase t (m)	0.5
Height of roll center h (m)	0.5	–	–

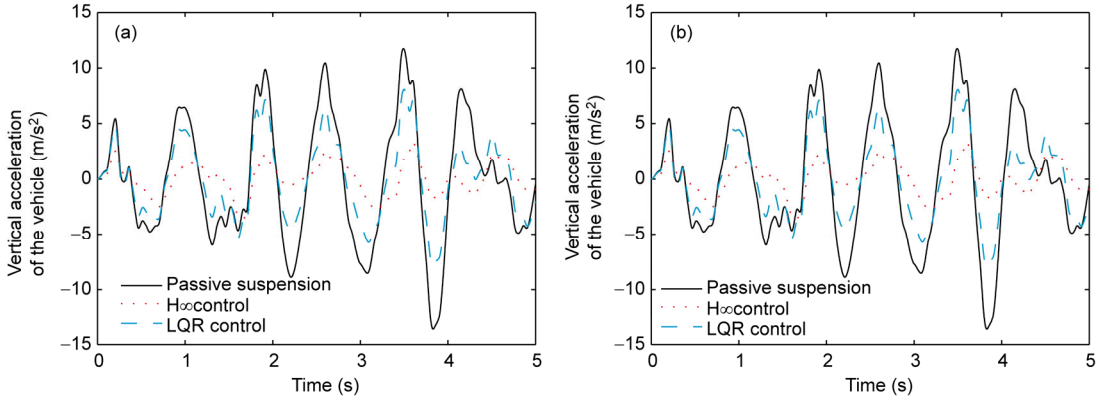

Figure 6 (Color online) Vertical acceleration of the vehicle. (a) δ=6°; (b) δ=10°.

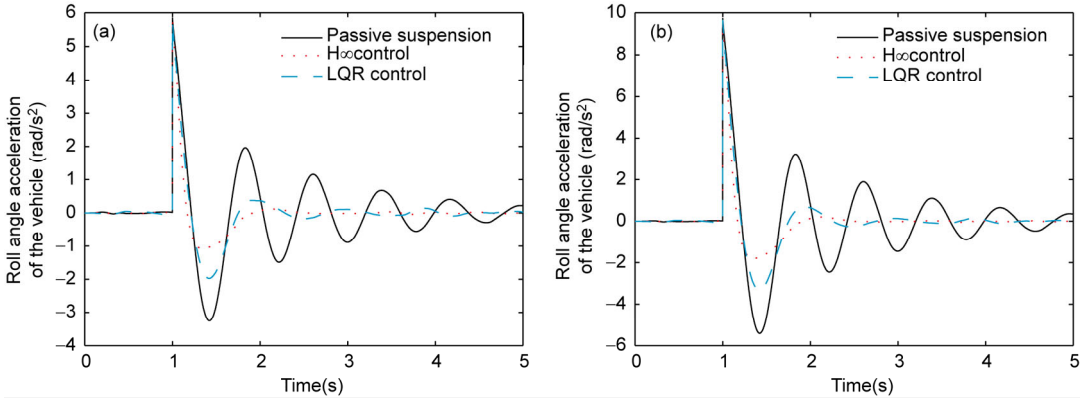

Figure 7 (Color online) Roll angle acceleration of the vehicle. (a) δ=6°; (b) δ=10°.

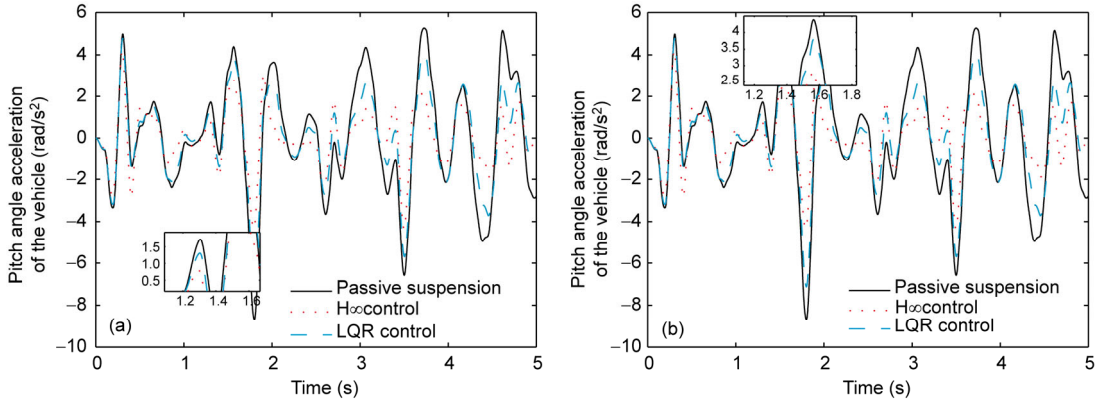

Figure 8 (Color online) Pitch angle acceleration of the vehicle. (a) δ=6°; (b) δ=10°.

have little differences. However, the roll angle acceleration and suspension dynamic deflection have large changes under the two front wheel angle inputs. The peak value of the front wheel angle with 6° is reduced by 40% than the one of 10°. Therefore, the vehicle's comfort and smoothness of the latter is slightly worse.

(3) Compared with LQR control, the vehicle vertical acceleration, roll angle acceleration, pitch angle acceleration and suspension dynamic deflection are all improved under H_∞ robust control, and the corresponding mean values are decreased by 22.4%, 6.3%, 32.7% and 12.4% respectively. Therefore, H_∞ robust control has a better control effect than LQR control at different front wheel angle. It can further improve the anti-roll capability of the vehicle and inhibit the changes of the body under steering condition.

4.2 Different road inputs simulation.

Setting the initial speed of the vehicle as 20 m/s and the front wheel angle δ as the step input of 8°, the simulations

are carried out under the road condition of *A*/*B*/*C*-class respectively. Figures 10–13 show the simulation results of the main performance of the passive suspension and the active suspension under different control.

It can be seen from Figures 10–13 that, compared with the passive suspension, the active suspension can reduce the vehicle vertical acceleration, roll angle acceleration, pitch angle acceleration and suspension dynamic deflection in different degrees. For example, the peak values of the vehicle vertical acceleration are decreased by 55% and 42% under H_∞ robust control and LQR control respectively. Moreover, in comparison with LQR control, the reduction with H_∞ robust control is even bigger, whose root-mean-square of the vehicle vertical acceleration, roll angle acceleration, pitch angle acceleration and suspension dynamic deflection are reduced by 10.6%, 75%, 57.4% and 8.8% respectively. Therefore, H_∞ robust control has a better control effect than LQR control in different road conditions. In addition, under H_∞ robust control, the vehicle vertical acceleration and suspension dynamic deflection at *A*-class

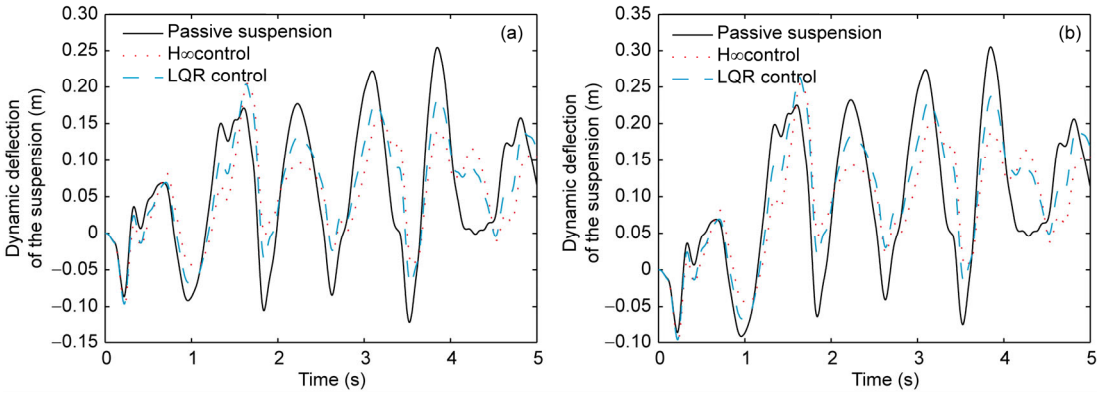

Figure 9 (Color onine) Dynamic deflection of the suspension. (a) δ=6°; (b) δ=10°.

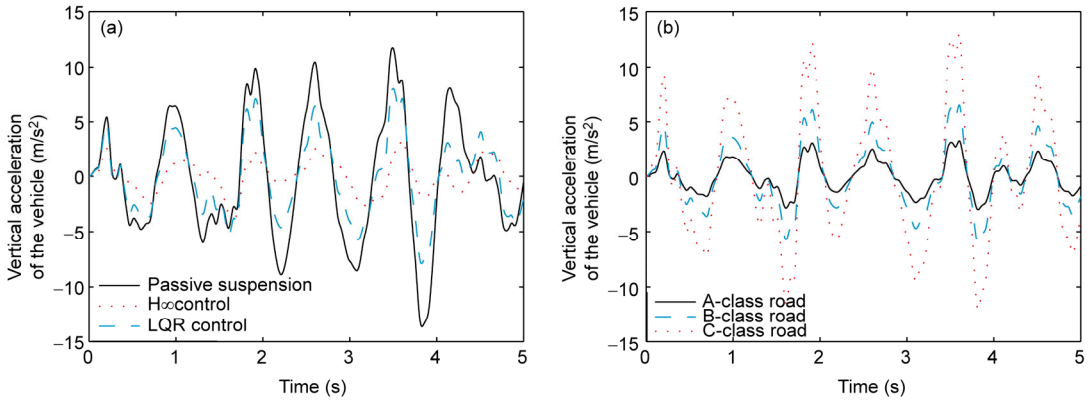

Figure 10 (Color online) Vertical acceleration of the vehicle. (a) *B*-class road; (b) *A*/*B*/*C*-class road (H_∞ robust control).

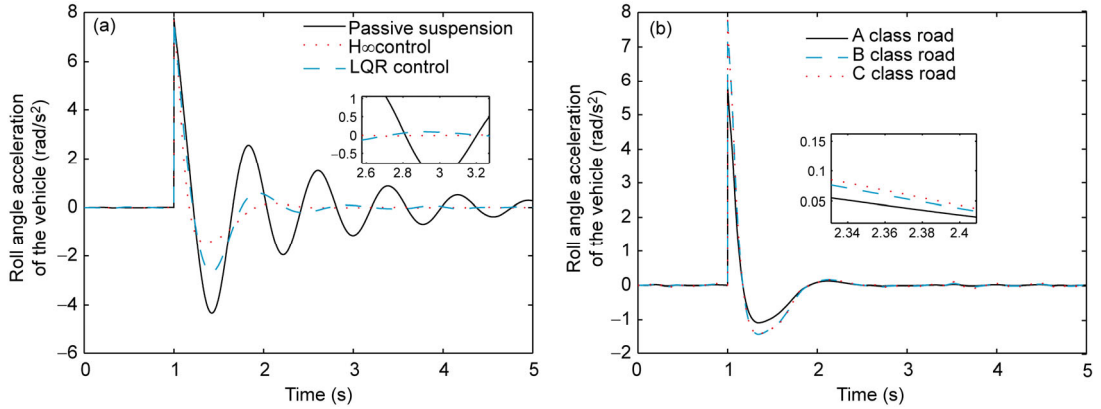

Figure 11 (Color online) Roll angle acceleration of the vehicle. (a) *B*-class road; (b) *A*/*B*/*C*-class road (H_∞ robust control).

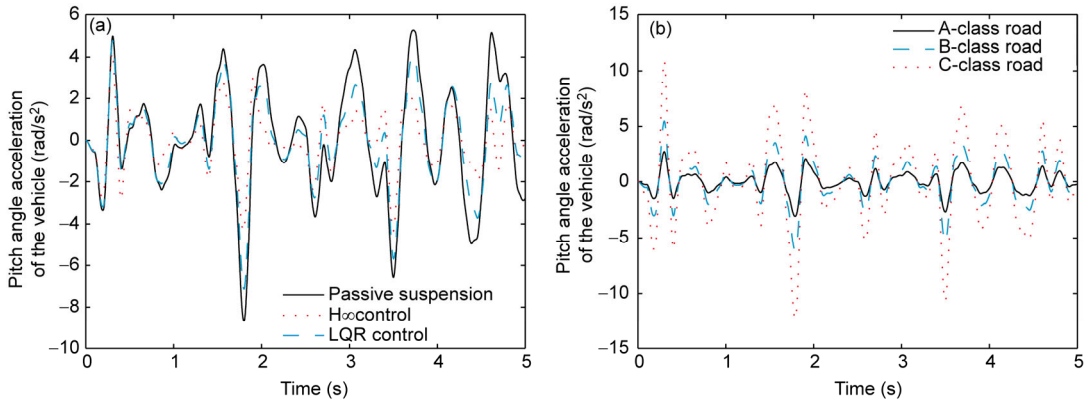

Figure 12 (Color online) Pitch angle acceleration of the vehicle. (a) *B*-class road; (b) *A*/*B*/*C*-class road (H_∞ robust control).

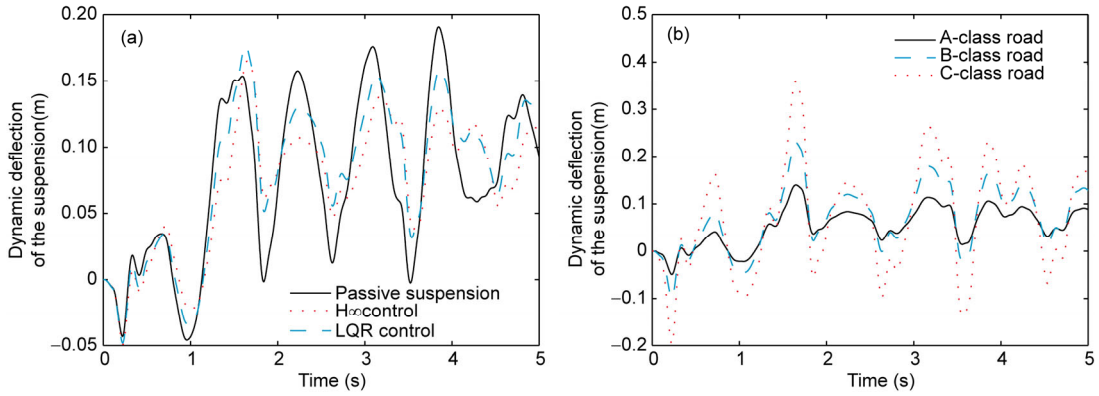

Figure 13 (Color online) Dynamic deflection of the suspension. (a) *B*-class road; (b) *A*/*B*/*C*-class road (H_∞ robust control).

road are much smaller than *C*-class road, which shows it has a better riding comfort and smoothness at the *A*-class road. However, the roll angle accelerations at the three road conditions don't have much difference, which indicates the pitching motion is effectively restrained with the designed H_∞ robust controller. In summary, the active suspension with H_∞ robust controller can inhibit the body changes in different road conditions, and improve the riding comfort of the vehicle.

4.3 Amplitude-frequency characteristic simulation

In order to analyze the amplitude frequency characteristics of the system with H_∞ controller in different frequency bands, the frequency domain simulations are conducted. Setting the initial speed of the vehicle as 20 m/s, the front wheel angle δ as 6°, and the road condition as *B*-class, the simulation results of passive suspension, active suspension with H_∞ and LQR controller are shown in Figures 14–17.

Figures 14–17 show the Bode diagram of the vehicle vertical acceleration, roll angle acceleration, pitch angle acceleration and suspension dynamic deflection to the road input at the left front wheel. It can be seen from Figures 14–17 that the amplitude frequency characteristic of the active suspension with LQR controller has little difference compared with the passive suspension. However, it differs a lot with H_∞ controller. The amplitudes of the roll angle acceleration and pitch angle acceleration under H_∞ controller are decreased obviously in human body sensitive frequency segment of 1–10 Hz, and it is the same as the vehicle vertical acceleration in the frequency range of 4–8 Hz. Therefore, the designed H_∞ controller can significantly improve the riding comfort of the active suspension system in the sensi-

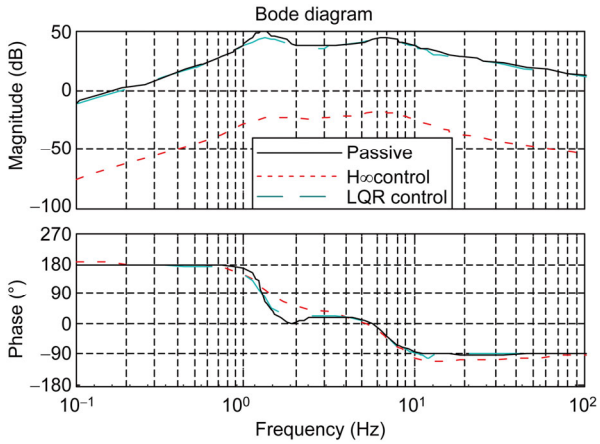

Figure 14 (Color online) Vertical acceleration of the vehicle.

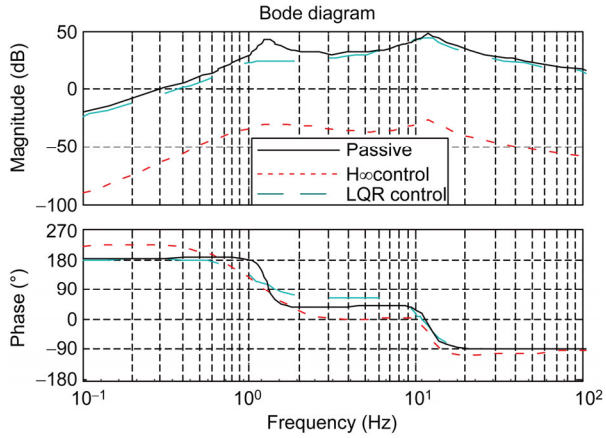

Figure 15 (Color online) Roll angle acceleration of the vehicle.

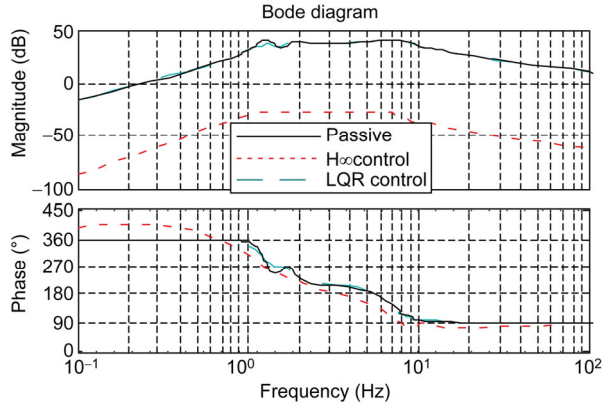

Figure 16 (Color online) Pitch angle acceleration of the vehicle.

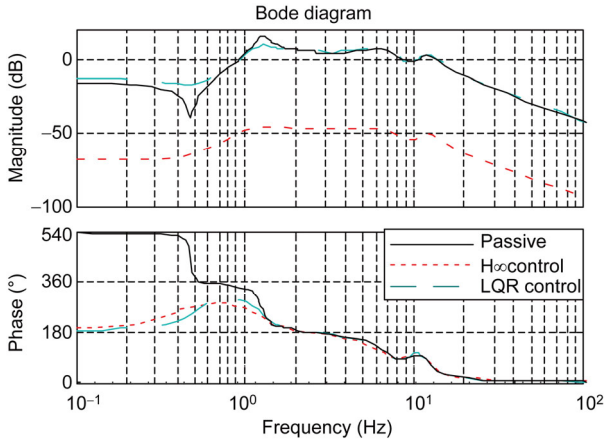

Figure 17 (Color online) Dynamic deflection of the suspension.

tive frequency range for human body.

5 Steering wheel angle step input test

The steering wheel angle step input test is mainly used to verify the comprehensive performance of the vehicle. The test is conducted according to GB/T6323.2-94: vehicle handling stability test method-steering transient test. In the test, the speed of the vehicle is set to 40 km/h, and the steering wheel angle input is 90° step input, which meet the requirements of the jump time. Test results as shown in Table 2.

It can be seen from Table 2 that compared with the passive suspension system, the active suspension with H_∞ robust controller can better inhibit the auto body's posture change under steering condition, and improve the comprehensive performance of the vehicle. The peak value and standard deviation of the yaw rate are decreased by 2.16% and 5.16%, and the ones of roll angle are reduced by 15.89% and 8.19%, and the corresponding ones of vertical acceleration of center of mass are declined by 28.57% and 27.75%. Therefore, the active suspension system with the proposed controller can significantly improve the riding comfort and handling stability.

6 Conclusions

In this paper, the dynamic model of the active suspension system is established under steering condition. Then, considering the vehicle's vibration of roll, acceleration and pitch motion etc., in the steering process, the H_∞ robust controller is designed based on generalized system with frequency weighting, which considers the sensitive vibrationfrequency range of the human body. The simulations under steering condition are carried out with different front wheel angles, random road inputs and amplitude-frequency characteristic. To verify the control effect, the active suspension with H_∞ robust controller is compared with LQR controller and the passive suspension. Simulation results show that, in comparison with the passive suspension, the active suspension can efficiently reduce the vehicle vertical acceleration, roll angle acceleration, pitch angle acceleration and suspension dynamic deflection. So it can better buffer the vibration impact from the road, and improve the riding comfort of the vehicle. Moreover, H_∞ robust control has a better control effect than LQR control. The active suspension with H_∞ robust controller can further improve the anti-roll capability of the vehicle, and inhibit the changes of

Table 2 Test results

Performance index	Passive suspension		Robust control suspension		Performance improvement (%)	
	Peak value	Standard deviation	Peak value	Standard deviation	Peak value	Standard deviation
Yaw rate ω (rad s^{-1})	0.6256	0.1284	0.5619	0.1121	2.16	5.16
Roll angle θ (rad)	–0.1114	0.1051	–0.0962	0.1002	15.80	8.19
Vertical acceleration Z_S (m s^{-2})	5.400	1.832	4.200	1.434	28.57	27.75

the body under steering condition. Especially in human body's sensitive frequency segments, the amplitudes of the roll angle acceleration and pitch angle acceleration under H_∞ controller are decreased obviously. In addition, the steering wheel angle step input test is carried out, which verifies the comprehensive performance of the vehicle. The results of this study provided certain theoretical basis for research and application of the active suspension system.

This work was supported by the Fundamental Research Funds for the Central Universities (Grant No. NS2015020).

1 Yao G Z, Yap F F, Chen G. MR damper and its application for semi-active control of vehicle suspension system. Mechatronics, 2002, 12: 963–973
2 Capitani R, Masi G, Meneghin A, et al. Handling analysis of two-wheel vehicle using MSC. ADAMS/Motorcycle. Veh Syst Dyn, 2006, 44: 698–707
3 Yoshimura T, Nakaminami K. Active suspension of passenger cars using linear and fuzzy-logic controls. Control Eng Practice, 1999, 7: 41–47
4 Kalaivani R, Lakshmi P, Sudhagar K. Vibration control of vehicle active suspension system using novel fuzzy logic controller. Int J Enterp Netw Manage, 2014, 6: 139–152
5 Kurczyk S, Pawelczyk M. Fuzzy control for semi-active vehicle suspension. J Low Frequency Noise Vib Act Control, 2013, 32: 217–225
6 Luo X, Li J. Fuzzy dynamic characteristic model based attitude control of hypersonic vehicle in gliding phase. Sci China Inf Sci, 2011, 54: 448–459
7 Li H B, Sun Z Q, Min H B, et al. Fuzzy dynamic characteristic modeling and adaptive control of nonlinear systems and its application to hypersonic vehicles. Sci China Inf Sci, 2011, 54: 460–468
8 Yoshimura T, Teramura I. Active suspension system for a one-wheel car model using single input rule modules fuzzy reasoning. Int J Veh Auton Syst, 2004, 1: 237–255
9 Wu S J, Chiang H H, Chen J H, et al. Optimal fuzzy control design for half-car active suspension systems. In: Proceeding of the 2004 IEEE International Conference on Networking, Sensing & Control. Taipei: IEEE, 2004. 583–588
10 Sadati S H, Malekzadeh S, Ghasemi M. Optimal control of an 8-DOF vehicle active suspension system using Kalman observer. Shock Vib, 2008, 15: 493–503
11 Tina P, Alessandro G, Cerla S. Constrained optimal control: An application to semi-active suspension systems. Int J Syst Sci, 2010; 41: 797–811
12 MarLbanrad J, Abroad G, Zohoor H, et al. Stochastic optimal preview control of a vehicle suspension. J Sound Vib, 2004, 27: 973–990
13 Khiavi A M, Mirzaei M, Hajimohammadi S. A new optimal control law for the semiactive suspension system considering the nonlinear magneto-rheological damper model. J Vib Control, 2013, 20: 2221–2233
14 Fateh M M, Zirkohi M M. Adaptive impedance control of a hydraulic suspension system using particle swarm optimization. Veh Syst Dyn-Int J Veh Mech Mobility, 2011, 49: 1951–1965
15 Huang Y B, Jing N, Wu X, et al. Adaptive control of nonlinear uncertain active suspension systems with prescribed performance. ISA Trans, 2015, 54: 145–155
16 Zhao W Z, Wang C Y, Zhao T, et al. Research on the multi- disciplinary design method for an integrated automotive steering and suspension system. Proc Inst Mech Eng, Part D-J Automob Eng, 2015, 229: 1249–1262
17 Lu Y J, Yang S P, Li S H. Research on dynamics of a class of heavy vehicle-tire-road coupling system. Sci China Tech Sci, 2011, 54: 2054–2063
18 Jia G, Li L, Cao D. Model-based estimation for vehicle dynamics states at the limit handling. J Dyn Syst Meas Control, 2015, 137: 1–8
19 Sun W, Gao H, Kaynak O. Finite frequency H_∞ control for vehicle active suspension systems. IEEE Trans Control Syst Tech, 2011, 19: 416–422
20 Sun W, Zhao Y, Li J, et al. Active suspension control with frequency band constraints and actuator input delay. IEEE Trans Ind Electron, 2012, 59: 530–537
21 Chen Y K, Jie H E, Mark K, et al. Effect of driving conditions and suspension parameters on dynamic load-sharing of longitudinal-connected air suspensions. Sci China Tech Sci, 2013, 56: 666–676
22 Choi S B, Lee H S, Park Y P. H_∞ control performance of a full-vehicle suspension featuring magneto-rheological dampers. Veh Sys Dyn, 2002, 8: 355–360
23 Lauwerys C, Swevers J, Sas P. Robust linear control of an active suspension on a quarter car test-rig. Control Eng Pract, 2005; 13: 577–586
24 Shimomura T, Fuji T. Subspace controller design to the mixed H_2/H_∞ synthesis with uncommon LMI solutions. In: Proceedings of the American Control Conference. Philadelphia: IEEE, 1998. 547–549
25 Wang J, Wilson D A, Halikias G D. H_∞ robust-performance control of decoupled active suspension systems based on LMI method. In: Proceedings of the American Control Conference. Arlington: IEEE, 2001. 2658–2663